Hamburger Beiträge
zur Angewandten Mathematik

A note on variational discretization of elliptic Neumann boundary control

Michael Hinze and Ulrich Matthes

Nr. 2008-01
January 2008

A note on variational discretization of elliptic Neumann boundary control

Michael Hinze*& Ulrich Matthes†

January 14, 2008

Abstract: We consider variational discretization of Neumann-type elliptic optimal control problems with constraints on the control. In this approach the cost functional is approximated by a sequence of functionals which are obtained by discretizing the state equation with the help of linear finite elements. The control variable is not discretized. Optimal error bounds for control and state are obtained both in two and three space dimensions. Finally, we discuss some implementation issues of a generalized Newton method applied to the numerical solution of the problem class under consideration.

Mathematics Subject Classification (2000): 49J20, 49K20, 35B37

Keywords: Elliptic optimal control problem, error estimates, Neumann boundary control, variational discretization.

1 Introduction

Let $\Omega \subset \mathbb{R}^d$ $(d = 2, 3)$ be a bounded domain with a smooth boundary $\partial\Omega$. In this note, we are interested in the following control problem:

$$\begin{aligned} &\min_{w\in U} J(w) = \tfrac{1}{2}\int_\Omega |\mathcal{G}(Bw) - y_0|^2 + \tfrac{\alpha}{2}\|w\|_U^2 \\ &\text{subject to } w \in U_{ad}. \end{aligned} \tag{1.1}$$

We suppose that $\alpha > 0$ are given. Further $(U, (\cdot,\cdot)_U)$ denotes a Hilbert space which we identify with its dual, and $B : U \to (H^1(\Omega))'$ a linear, continuous operator, and $U_{ad} \subseteq U$ denotes the closed, convex set of admissible controls. Furthermore, for given $f \in (H^1(\Omega))'$ the function $\mathcal{G}(f)$ denotes the unique weak solution $y \in H^1(\Omega)$ to the elliptic boundary value problem

$$a(y, v) = \langle f, v\rangle \quad \forall\ v \in H^1(\Omega). \tag{1.2}$$

Here, $\langle\cdot,\cdot\rangle$ denotes the dual pairing of $H^1(\Omega)'$ and $H^1(\Omega)$, the bilinear form a is defined by

$$a(y, v) := \int_\Omega \Big(\sum_{i,j=1}^d a_{ij}(x) y_{x_i} v_{x_j} + \sum_{i=1}^d b_i(x) y_{x_i} v + c(x) yv\Big) dx,$$

where we assume that the coefficients $a_{i,j}, b_i$ and c are sufficiently smooth and chosen such that the form is H^1-coercive with constant $c_1 > 0$. Finally, $\Gamma := \partial\Omega$.

*Schwerpunkt Optimierung und Approximation, Universität Hamburg, Bundesstraße 55, 20146 Hamburg, Germany.

†Institut für Numerische Mathematik, TU Dresden, Zellescher Weg 12-14, 01062 Dresden, Germany

Now, it is not hard to prove that problem (1.1) admits a unique solution $u \in U_{ad}$. Moreover, there exists a function $p \in H^1(\Omega)$ which together with $y = \mathcal{G}(Bu)$ satisfies

$$a(v,p) = \int_\Omega (y - y_0)v \ \forall v \in H^1(\Omega) \tag{1.3}$$

$$(B^*p + \alpha u, q - u)_U \geq 0 \quad \text{for all } q \in U_{ad}, \tag{1.4}$$

Example 1.1. There are several examples for the choice of B and U.

(i) Distributed control: $U = L^2(\Omega)$, $B = Id : L^2(\Omega) \to H^1(\Omega)'$.

(ii) Boundary control: $U = L^2(\Gamma)$, $Bu(\cdot) = \int_\Gamma u\gamma_0(\cdot)\, dx : L^2(\Omega) \to H^1(\Omega)'$, where γ_0 is the trace operator in $H^1(\Omega)$.

(iii) Linear combinations of input fields: $U = \mathbb{R}^n$, $Bu = \sum_{i=1}^n u_i f_i$, $f_i \in H^{-s}(\Omega)$, $s < (d-1)/d$.

From here onwards we consider Example 1.1(ii).

A finite element analysis for general semilinear elliptic Neumann boundary control problems on two-dimensional polygonal convex domains is provided by Casas and Mateos in [2]. Among other things they prove $\|u - u_h\|_{L^2(\Gamma)} = o(h)(h \to 0)$ for a piecewise linear, continuous finite element approximation u_h of u, and, for cost functionals with quadratic structure in the control part, $\|u - u_h\|_{L^2(\Gamma)} = O(h^{3/2-\epsilon})(h \to 0)$ for the variational discretization u_h, where in both cases $u \in U_{ad}$ denotes a solution to the corresponding optimal control problem.
Here we provide results for two- and three-dimensional domains and provide optimal error estimates in $L^2(\Gamma)$ and $L^\infty(\Gamma)$ for variational discretizations of problem (1.1). We use a general proof technique which differs from that applied in [2]. We concentrate on linear-quadratic optimal control problems since the essential nonlinearity from the point of view of optimization is introduced through the constraint $u \in U_{ad}$ in terms of the orthogonal projection associated with this constraint.
Let us comment on further approaches that tackle optimization problems for pdes with constrained boundary controls. In [3] a problem similar to that of [2] is studied and piecewise constant approximations for the control are investigated. In [1] Dirichlet boundary control for semilinear elliptic control problems is considered for convex polygonal domains in two dimensions. Finally, [12] proves h^2 convergence for superpositions of smooth Dirichlet boundary control actions for linear-quadratic optimal control problems.
The rest of the paper is organized as follows: In Section 2 we collect basic results on (1.1). In Section 3 we present the finite element analysis of problem (1.1). Among other aspects we show that bounds

$$\|u - u_h\|_{L^2(\Gamma)} \sim \|p - p^h(u)\|_{L^2(\Gamma)} + \|y - y^h(u)\|$$

where u_h denotes the unique solution to (3.6) and y^h, p^h denote finite element approximations to the optimal state y and to the adjoint state p associated to u, respectively. In Section 5 we describe the numerical implementation of the semi-smooth Newton algorithm for the problem class under consideration and present numerical results which confirm our theoretical findings. Semi-smooth Newton methods for elliptic and parabolic variational discrete control problems are investigated in [9].

2 The continuous problem

Since problem (1.1) is a convex it admits a unique solution $u \in U_{ad}$ with unique associated state $y = \mathcal{G}(Bu)$ and unique adjoint p. Crucial for the finite element analysis is the regularity

of the involved state, adjoint, and control. From here onwards let us assume that $U_{ad} = \{v \in L^2(\Gamma); a \leq v \leq b \text{ a.e. in } \Gamma\}$, where for simplicity $a < b$ denote constants (or sufficiently smooth, bounded functions). From (1.4) we deduce that u satisfies

$$u = P_{U_{ad}}\left(-\frac{1}{\alpha}B^* p\right), \tag{2.5}$$

where B^* denotes the adjoint of B, and in the present setting coincides with the trace operator, and the action of the orthogonal projection $P_{U_{ad}} : U \to U_{ad}$ is given by

$$P_{U_{ad}}(f)(x) = \max\{a, \min\{f(x), b\}\}.$$

Since $\max, \min$ are Lipschitz continuous functions we may at best expect Lipschitz continuity of $P_{U_{ad}}(f)$, regardless how smooth the function f is. Thus, a bootstrapping argument at best yields $u \in W^{1,\infty}(\Gamma)$ with corresponding state $y \in W^{2,s}(\Omega)$ and adjoint $p \in W^{4,s}(\Omega)$ for all $1 \leq s < \infty$. In the case of a convex polygonal domain both the regularity of y and p is further restricted to $y \in W^{2,s_0}(\Omega)$ for some $d \leq s_0 < \infty$, and $p \in W^{2,s}(\Omega)$ for some $d \leq s < \infty$.

3 Finite element discretization and error analysis for (1.1)

Let $\mathcal{T}_h$ be a triangulation of Ω with maximum mesh size $h := \max_{T\in\mathcal{T}_h} \operatorname{diam}(T)$ and vertices $x_1, \ldots, x_m$. We suppose that $\bar{\Omega}$ is the union of the elements of $\mathcal{T}_h$ so that element edges lying on the boundary are curved. In addition, we assume that the triangulation is quasi-uniform in the sense that there exists a constant $\kappa > 0$ (independent of h) such that each $T \in \mathcal{T}_h$ is contained in a ball of radius $\kappa^{-1}h$ and contains a ball of radius κh. Let us define the space of linear finite elements,

$$X_h := \{v_h \in C^0(\bar{\Omega}) \,|\, v_h \text{ is a linear polynomial on each } T \in \mathcal{T}_h\}$$

with the appropriate modification for boundary elements.
In what follows it is convenient to introduce a discrete approximation of the operator $\mathcal{G}$. In fact, for a given function $f \in H^1(\Omega)'$ we denote by $z_h = \mathcal{G}_h(f) \in X_h$ the solution of the discrete Neumann problem

$$a(z_h, v_h) = \langle f, v_h\rangle \text{ for all } v_h \in X_h.$$

Problem (1.1) is now approximated by the following sequence of control problems depending on the mesh parameter h:

$$\min_{u\in U_{ad}} J_h(u) := \frac{1}{2}\int_\Omega |\mathcal{G}_h(Bu) - y_0|^2 + \frac{\alpha}{2}\|u\|_U^2. \tag{3.6}$$

Problem (3.6) represents a convex infinite-dimensional optimization problem of a similar structure as problem (1.1). It admits a unique solution $u_h \in U_{ad}$ with corresponding state $y_h \in X_h$. Furthermore, in accordance with problem (1.1), there exist a unique function $p_h \in X_h$ satisfying

$$a(v_h, p_h) = \int_\Omega (y_h - y_0)v_h \text{ for all } v_h \in X_h, \text{ and} \tag{3.7}$$

$$(\alpha u_h + B^* p_h, v - u_h)_U \geq 0 \text{ for all } v \in U_{ad}. \tag{3.8}$$

Moreover

$$u_h = P_{U_{ad}}\left(-\frac{1}{\alpha}B^* p_h\right). \tag{3.9}$$

We note that the control is not discretized in (3.6), which is reflected by the appearance of the orthogonal projector $P_{U_{ad}}$ in (3.9), compare [7, 8] for a more detailed discussion of this discretization approach.
Next we prove a general error estimate in h.

Theorem 3.1. Let u denote the solution of (1.1) with $y = \mathcal{G}(Bu)$, and u_h the solution to (3.6) with $y_h = \mathcal{G}_h(Bu_h)$. Then

$$\alpha\|u - u_h\|_U^2 + \|y - y_h\|^2 \leq C_\alpha\|p - p^h\|_{L^2(\Gamma)}^2 + \|y - y^h\|^2, \tag{3.10}$$

where y^h, p^h denote the unique solutions to $a(y^h, v_h) = \langle Bu, v_h\rangle$, and $a(v_h, p^h) = \int_\Omega (y - y_0)v_h$ for all $v_h \in X_h$.

Proof. We use u_h as test function in (1.4), u as test function in (3.7) and add the resulting variational inequalities. This yields

$$\begin{aligned}\alpha\|u - u_h\|_U^2 \leq \langle B(u_h - u), p - p_h\rangle &= \langle B(u_h - u), p - p^h\rangle + \langle B(u_h - u), p^h - p_h\rangle \leq \\ &\leq \|B^*(p - p^h)\|_U\|u - u_h\|_U + a(y_h - y^h, p^h - p_h) = \\ &= \|B^*(p - p^h)\|_U\|u - u_h\|_U + \int_\Omega (y - y_h)(y_h - y^h) \leq \\ &\leq \|B^*(p - p^h)\|_U\|u - u_h\|_U - \frac{1}{2}\|y - y_h\|^2 + \frac{1}{2}\|y - y^h\|^2.\end{aligned}$$

Since B^* coincides with the trace operator we obtain with the help of Young's inequality

$$\alpha\|u - u_h\|_U^2 + \|y - y_h\|^2 \leq C_\alpha\|p - p^h\|_{L^2(\Gamma)}^2 + \|y - y^h\|^2.$$

This completes the proof.
Next we prove L^∞ error estimates for the optimal controls.

Theorem 3.2. Let u denote the solution of (1.1) with $y = \mathcal{G}(Bu)$, and u_h the solution to (3.6) with $y_h = \mathcal{G}_h(Bu_h)$. Then

$$\|u - u_h\|_{L^\infty(\Gamma)} \leq C\left\{\|p - p^h\|_{L^\infty(\Gamma)} + \gamma(h)\|y - y^h\|\right\}, \tag{3.11}$$

where $\gamma(h) = |\ln h|$ for $d = 2$, and $\gamma(h) = h^{-1/2}$ for $d = 3$.

Proof. With the help of (2.5),(3.9) we obtain

$$\begin{aligned}\|u - u_h\|_{L^\infty(\Gamma)} = \|P_{U_{ad}}(-\frac{1}{\alpha}B^*p) - P_{U_{ad}}(-\frac{1}{\alpha}B^*p_h)\|_{L^\infty(\Gamma)} &\leq \frac{1}{\alpha}\|p - p_h\|_{L^\infty(\Gamma)} \leq \\ &\leq \frac{1}{\alpha}\|p - p^h\|_{L^\infty(\Omega)} + \frac{1}{\alpha}\|p^h - p_h\|_{L^\infty(\Omega)} \leq \\ &\leq \frac{1}{\alpha}\|p - p^h\|_{L^\infty(\Omega)} + \gamma(h)\|p^h - p_h\|_{H^1(\Omega)},\end{aligned}$$

where $\gamma(h) = |\ln h|$ for $d = 2$, and $\gamma(h) = h^{-1/2}$ for $d = 3$, see [13]. We proceed with estimating $\|p^h - p_h\|_{H^1(\Omega)}$ according to

$$\|p^h - p_h\|_{H^1(\Omega)}^2 \leq Ca(p^h - p_h, p^h - p_h) \leq C\|p^h - p_h\|\|y - y_h\|.$$

This completes the proof.
From the estimates (3.10) and (3.11) we deduce that the approximation quality of the control is steered by the approximation quality of finite element solutions y^h to the state y, and by the finite element approximation p^h of the adjoint p.
Let us consider some examples.

Example 3.3. 1. Let us consider the situation of [2, Section 5,6], where Ω is a two-dimensional convex polygonal domain, i.e. $d = 2$. Further let $y_0 \in L^2(\Omega)$. Then $y, p \in H^2(\Omega)$, so that by [2, Theorem 4.1] we have $\|y - y^h\| \le Ch^2$ and $\|p - p^h\|_{L^2(\Gamma)} \le h^{3/2}$. Thus, (3.10) directly yields

$$\|u - u_h\|_{L^2(\Gamma)} \le Ch^{3/2}.$$

2. Let us consider a smooth, bounded two- or three-dimensional domain Ω and let the approximation properties A1-A4 of [10] be satisfied. Bootstrapping yields at least $y \in H^2(\Omega)$ and $p \in H^4(\Omega) \hookrightarrow W^{2,\infty}(\Omega)$ for $d < 4$. Thus we deduce from [10, Theorem 2.2]

$$\|p - p^h\|_\infty \le Ch^{2-\frac{d}{q}} |\log h| \|p\|_{W^{2,q}} \text{ for all } d \le q \le \infty,$$

compare also [4, Lemma 3.4], and again $\|y - y^h\| \le Ch^2$. Thus, (3.11) directly delivers

$$\|u - u_h\|_{L^\infty(\Gamma)} \le C \left\{ h^{2-\frac{d}{q}} |\log h| + \gamma(h) h^2 \right\} \text{ for all } d \le q \le \infty.$$

We should note that when using finite element approximations defined over partitions formed of simplexes one has to consider also an error induced by boundary approximations. However, locally, for small enough gridsizes the smooth boundary may be parametrized as graph over the faces of the corresponding simplex. For smooth boundaries the difference of the areas of the face and the corresponding graph is bounded by the square of the gridsize, so that error estimates of the same quality as in this example also hold for the accordingly transformed continuous solution, see [5].

4 Semismooth Newton algorithm

To solve problem (3.6) numerically we apply a semi-smooth Newton algorithm to the equation

$$G(u) := u - P_{U_{ad}}(-\frac{1}{\alpha} B^* p_h(u)) = 0 \text{ in } U, \tag{4.12}$$

where for given $u \in U$ with associated discrete state $y_h(u)$ the function $p_h(u)$ solves (3.7). It follows from (2.5) that this equation in our setting admits the unique solution $u_h \in U_{ad}$ of problem (3.6). Moreover, it directly follows with the results of [6, 11] that G is semi-smooth in the sense that

$$\sup_{M \in \partial G(u+s)} \|G(u+s) - G(u) - Ms\|_U = o(\|s\|_U) \text{ as } \|s\|_U \to 0,$$

where

$$\partial G(u) := \left\{ I + D(u)(\frac{1}{\alpha} B^* p_h'(u)) \right\} \text{ with } D(u)(x) = \begin{cases} 0, & \text{if } -\frac{1}{\alpha} B^* p_h(u)(x) \notin [a,b] \\ \in [0,1], & \text{if } -\frac{1}{\alpha} B^* p_h(u)(x) \in \{a,b\} \\ 1, & \text{if } -\frac{1}{\alpha} B^* p_h(u)(x) \in (a,b) \end{cases}$$

denotes the generalized differential. With $g \equiv g(u)$ denoting the indicator function of the inactive set $\mathcal{I}(u) := \{x \in \Gamma; -\frac{1}{\alpha} B^* p_h(u)(x) \in (a,b)\}$ we set

$$G'(u) := I + \frac{1}{\alpha} g B^* p_h'(u) \in \partial G(u).$$

It follows from the considerations related to (4.16) that $G'(u)$ is bounded invertible, since $p_h'(u) = S_h^* S_h B$ with S_h denoting the finite element solution operator. Thus, $B^* p_h'(u) = B^* S_h^* S_h B$ is positive semi-definite on U.
We are now in the position to formulate

Algorithm 4.1. Semi-smooth Newton algorithm
Choose $u \in U$
While $G(u) \neq 0$ solve

$$G'(u)u^{new} = G'(u)u - G(u) \tag{4.13}$$

for u^{new} and set $u = u^{new}$.

We emphasize that this algorithm works in the infinite-dimensional space U so that it is not obvious that this algorithm is numerically implementable. For a related discussion we refer to [7].
Using

$$\beta := (I-g)\text{bounds} \equiv \begin{cases} a, & \text{if } -\frac{1}{\alpha}B^*p_h(u) < a \\ b, & \text{if } -\frac{1}{\alpha}B^*p_h(u) > b \\ 0, & \text{else} \end{cases}$$

a short calculation shows, that the Newton equation (4.13) can be rewritten in the form

$$u^{new} = \text{bounds on } \mathcal{A}(u) := \Gamma \setminus \mathcal{I}(u), \text{ and} \tag{4.14}$$

$$(\alpha g I + gB^*S_h^*S_hBg)u^{new} = -gB^*(S_h^*y_0 - S_h^*S_hB\beta). \tag{4.15}$$

We solve the equation

$$(\alpha g I + gB^*S_h^*S_hBg)u^{new} = -gB^*(S_h^*y_0 - S_h^*S_hB\beta)$$

with a conjugate gradient method. This is feasible since for given $u \in U$ the operator $\mathcal{E}_I^*(\alpha I + B^*S_h^*S_hB)\mathcal{E}_I$ is positive definite on $L^2(\mathcal{I}(u))$, where the function $\mathcal{E}_I f \in L^2(\Gamma)$ denotes the extension-by-zero to Γ of functions $f \in L^2(\mathcal{I}(u))$, and $\mathcal{E}_I^*$ denotes its adjoint whose action for $s \in L^2(\Gamma)$ is given by $\mathcal{E}_I^* s = (gs)_{|_{\mathcal{I}(u)}}$. Thus, formally solving (4.15),(4.14) corresponds to solving

$$\mathcal{E}_I^*(\alpha I + B^*S_h^*S_hB)\mathcal{E}_I u_I^{new} = -\mathcal{E}_I^*B^*(S_h^*y_0 - S_h^*S_hB\beta) \tag{4.16}$$

and then setting $u^{new} = u_I^{new}$ on $\mathcal{I}(u)$, and $u^{new} =$ bounds on $\mathcal{A}(u)$, compare also [6, (4.7)]. It is now clear from these considerations that the Newton iterates may develop kinks or even jumps along the border of the active set, see the numerical results of the next section. However, it follows from the definition of the active set $\mathcal{A}(u)$ that its border consists of polygons, since we use continuous, piecewise linear ansatz functions for the state. We note that this border in general consists of piecewise polynomials of the same degree as that of the finite element ansatz functions, if higher order finite elements are used, compare [8]. Therefore, Algorithm 4.1 is numerically implementable, since in every of its iterations only a finite number of degrees of freedom has to be managed, which in the present case of linear finite elements can not exceed $3nv+2ne$, where nv denotes the number of finite element nodes, and ne the number of finite element edges, see [8, Chapter 3] and [7] for details. Moreover, the main ingredient of the cg algorithm applied to solve the Newton equation (4.16) consists in evaluating $\mathcal{E}_I^*(\alpha I + B^*S_h^*S_hB)\mathcal{E}_I f$ for functions $f \in L^2(\mathcal{I}(u))$. From the definitions of B and S_h it is then clear which actions have to be performed for this evaluation.
It is also clear, that only local convergence of the semi-smooth Newton algorithm can be expected, where the convergence radius at the solution depends on the penalization parameter α. For the numerical examples presented in the next section and the considered values of α it is sufficient use a cascadic approach where linear interpolations of numerical solutions on coarse grids are used as starting values on the next finer grid. Further details on the semi-smooth Newton methods applied to variationally discretized optimal control problems can be found in [9], where, among other things, also time-dependent problems are considered and globalization strategies are proposed.

5 Numerical experiments

We consider 2 numerical examples taken from [2] and compare the results of our numerical approach to the classical approach with piecewise linear, continuous ansatz functions for the controls taken there. For this purpose we define the experimental order of convergence by

$$eoc = \frac{\log E(h_1) - \log E(h_2)}{\log h_1 - \log h_2},$$

where $E(h)$ denotes an error functional an h the finite element grid size. There holds $eoc \sim \gamma$ if $E(h) \sim h^\gamma$.
In the examples investigated later there is an additional nonlinear function $e_u : \Gamma \to \mathbb{R}$ which makes the projection of nonlinear functions necessary.

$$u = P_{U_{ad}}(-\frac{1}{\alpha}(B^* p_h + e_u))$$

For the integration over the boundary control with kinks, we divide the boundary additionally to the division by the FEM discretization at the positions of the kinks. The kinks occur at prescribed points in e_u and at the intersections with the constraints. The latter are calculated with the Pegasus method (an improved regula-falsi method) because of the nonlinearity in e_u.

5.1 Example 1

is taken from Casas and Mateos [2, Section 7.1] and reads

$$\min \hat{J}(u) = \frac{1}{2}\int_\Omega (y_u(x) - y_\Omega)^2 dx + \frac{\alpha}{2}\int_\Gamma u(x)^2 dx + \int_\Gamma e_u(x)u(x)dx + \int_\Gamma e_y(x)y_u(x)dx$$

subject to $u \in U_{ad} = \{u \in L^2; 0 \le u(x) \le 1 \text{ a.e. } x \in \Gamma\}$, where y_u solves

$$\begin{aligned} -\Delta y_u(x) + c(x)y_u(x) &= e_1(x) && \text{in} \quad \Omega, \\ \partial_\nu y_u(x) + y_u(x) &= e_2(x) + u(x) && \text{on} \quad \Gamma. \end{aligned}$$

Here, $\Omega = (0,1)^2$, $\alpha = 1$, $c(x) = 1 + x_1^2 - x_2^2$, $e_y(x) = 1$, $y_\Omega(x) = x_1^2 + x_1 x_2$, $e_1(x) = -2 + (1 + x_1^2 - x_2^2)(1 + 2x_1^2 + x_1 x_2 - x_2^2)$,

$$e_u(x) = \begin{cases} -1 - x_1^3 & \text{on} \quad \Gamma_1 \\ -1 - \min \left\{ \begin{array}{l} 8(x_2 - 0.5)^2 + 0.58 \\ 1 - 16x_2(x_2 - y_1^*)(x_2 - y_2^*)(x_2 - 1) \end{array} \right\} & \text{on} \quad \Gamma_2 \\ -1 - x_1^2 & \text{on} \quad \Gamma_3 \\ -1 + x_2(1 - x_2) & \text{on} \quad \Gamma_4, \end{cases}$$

with $y_1^* = \frac{1}{2} - \frac{\sqrt{21}}{20}$ and $y_2^* = \frac{1}{2} + \frac{\sqrt{21}}{20}$. Further

$$e_2(x) = \begin{cases} 1 - x_1 + 2x_1^2 - x_1^3 & \text{on} \quad \Gamma_1 \\ 7 + 2x_2 - x_2^2 - \min\{8(x_2 - 0.5)^2 + 0.58, 1\} & \text{on} \quad \Gamma_2 \\ -2 + 2x_1 + x_1^2 & \text{on} \quad \Gamma_3 \\ 1 - x_2 - x_2^2 & \text{on} \quad \Gamma_4 \end{cases}$$

where Γ_1 to Γ_4 are the four edges of the unit square, numbered counterclockwise, starting with the bottom edge. The adjoint equation is given by

$$\begin{aligned} -\Delta\phi(x) + c(x)\phi(x) &= y_u(x) - y_\Omega(x) \quad \text{in} \quad \Omega \\ \partial_\nu\phi(x) + \phi(x) &= e_y(x) \quad \text{on} \quad \Gamma. \end{aligned}$$

An easy calculation shows that the optimal solution is given by

$$\bar{u}(x) = \begin{cases} x_1^3 & \text{on} \quad \Gamma_1 \\ \min\left\{8(x_2 - 0.5)^2 + 0.58, 1\right\} & \text{on} \quad \Gamma_2 \\ x_1^2 & \text{on} \quad \Gamma_3 \\ 0 & \text{on} \quad \Gamma_4, \end{cases}$$

with corresponding state $\bar{y}(x) = 1 + 2x_1^2 + x_1x_2 - x_2^2$ and adjoint state $\bar{\phi}(x) = 1$.
We note that in the numerical approach for this example (4.12) has to be replaced by

$$G(u) = u - P_{U_{ad}}(-\frac{1}{\alpha}(B^*p_h + e_u))$$

so that special attention caused by the nonlinearity appearing in e_u has to payed when evaluating $P_{U_{ad}}(-\frac{1}{\alpha}(B^*p_h(u) + e_u))$ for given u.
The errors and eocs are shown in table 1 for the Casas-Mateos-ansatz and the variational discretization respectively. The eoc of the numerical experiments of Casas and Mateos is calculated from tables of [2]. The eoc of the numerical experiments of Casas and Mateos is 1.5 and about 1.0 for the L^2 and L^∞ norm respectively. The eoc is 2 for our approach. This is better than expected by Example 3.3, 1. However, this may be caused by the special regularity of the continuous solution and the domain. The latter is polygonal but forms the limit case in regularity theory for elliptic domains with corners, so that also the estimate of Example 3.3 2. may apply. This would coincide with our numerical results. We further note that already the errors on the coarsest mesh for $h = 1$ are smaller in our approach than than those for $h = 2^{-4}$ or $h = 2^{-6}$ in the conventional Casas-Mateos-ansatz.
The Newton iteration is terminated if $\|G(u^i)\|/\|G(u^0)\| \leq 10^{-5}$ and $\|u^i - u^{i-1}\|/\max(\|u^i\|, \|u^{i-1}\|) \leq 10^{-5}$ holds. The inner cg iteration is terminated if $\|r\| \leq \frac{10^{-4}}{i}\min\left\{1, \|G(u^i)\|/, \|G(u^i)\|/\|G(u^0)\|\right\}$ holds with r denoting the current residuum of the Newton system.
In figure 1 the optimal control together with the error for $h = 0.5$ and the finite element grid is shown.

5.2 Example 2

is taken from Casas and Mateos [2, Section 7.2] and contains a semi-linear state equation instead of a linear one. It reads

$$\min \hat{J}(u) = \frac{1}{2}\int_\Omega (y_u(x) - y_\Omega)^2 dx + \frac{\alpha}{2}\int_\Gamma u(x)^2 dx + \int_\Gamma e_u(x)u(x)dx + \int_\Gamma e_y(x)y_u(x)dx$$

subject to $u \in U_{ad} = \left\{u \in L^2; 0 \leq u(x) \leq 1 \text{ a.e. } x \in \Gamma\right\}$, where y_u satisfies the semilinear equation

$$\begin{aligned} -\Delta y_u(x) + c(x)y_u(x) &= e_1(x) \quad \text{in} \quad \Omega \\ \partial_\nu y_u(x) + y_u(x) &= e_2(x) + u(x) - y(x)^2 \quad \text{on} \quad \Gamma. \end{aligned}$$

	Casas	Mateos	This	Paper	Casas	Mateos	This	Paper
h	$E_{u_{L^2}}$	$E_{u_{L^\infty}}$	$E_{u_{L^2}}$	$E_{u_{L^\infty}}$	$eoc_{u_{L^2}}$	$eoc_{u_{L^\infty}}$	$eoc_{u_{L^2}}$	$eoc_{u_{L^\infty}}$
2^{-0}	-	-	6.67e-3	5.03e-3	-	-	-	-
2^{-1}	-	-	2.27e-3	2.14e-3	-	-	1.55	1.23
2^{-2}	-	-	6.28e-4	5.72e-4	-	-	1.86	1.90
2^{-3}	-	-	1.62e-4	1.47e-4	-	-	1.95	1.96
2^{-4}	8.5e-3	4.1e-2	4.10e-5	3.73e-5	-	-	1.98	1.98
2^{-5}	3.0e-3	1.5e-2	1.03e-5	9.34e-6	1.5	1.5	1.99	2.00
2^{-6}	1.1e-3	1.1e-2	2.58e-6	2.34e-6	1.4	0.4	2.00	2.00
2^{-7}	3.7e-4	3.8e-3	6.44e-7	5.84e-7	1.6	1.5	2.00	2.00
2^{-8}	1.4e-4	2.7e-3	1.61e-7	1.46e-7	1.4	0.5	2.00	2.00
2^{-9}	-	-	4.03e-8	3.65e-8	-	-	2.00	2.00
2^{-10}	-	-	1.00e-8	9.09e-9	-	-	2.01	2.01

Table 1: Errors in u for the linear example

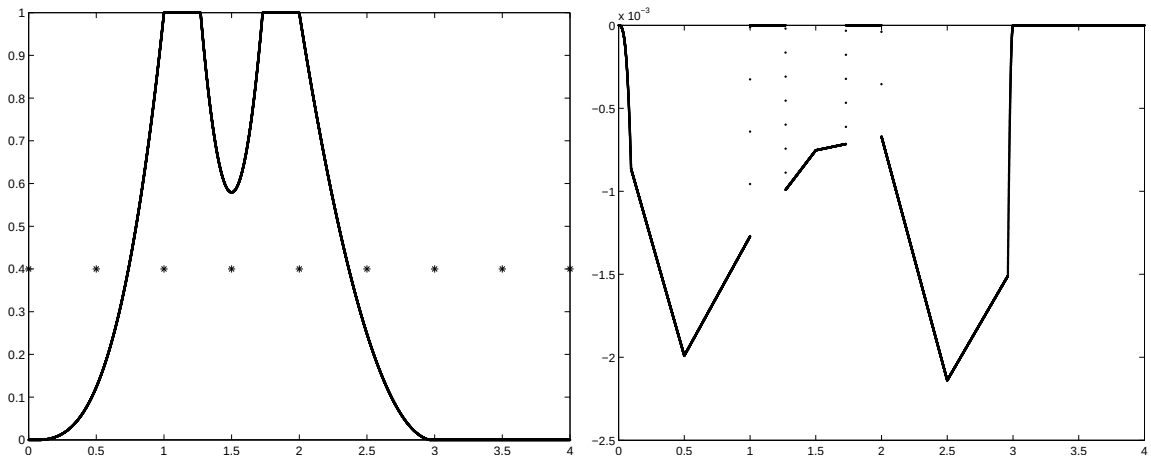

Figure 1: Optimal control u left, error in u right, both for $h = 0.5$.

Here, $\Omega = (0,1)^2$, $\alpha = 1$, $c(x) = x_2^2 + x_1 x_2$, $e_y(x) = -3 - 2x_1^2 - 2x_1 x_2$, $y_\Omega(x) = 1 + (x_1 + x_2)^2$, $e_1(x) = -2 + (1 + x_1^2 + x_1 x_2)(x_2^2 + x_1 x_2)$,

$$e_u(x) = \begin{cases} 1 - x_1^3 & \text{on} \quad \Gamma_1 \\ 1 - \min \left\{ \begin{array}{l} 8(x_2 - 0.5)^2 + 0.58 \\ 1 - 16 x_2 (x_2 - y_1^*)(x_2 - y_2^*)(x_2 - 1) \end{array} \right\} & \text{on} \quad \Gamma_2 \\ 1 - x_1^2 & \text{on} \quad \Gamma_3 \\ 1 + x_2(1 - x_2) & \text{on} \quad \Gamma_4, \end{cases}$$

with $y_1^* = \frac{1}{2} - \frac{\sqrt{21}}{20}$ and $y_2^* = \frac{1}{2} + \frac{\sqrt{21}}{20}$. Furthermore,

$$e_2(x) = \begin{cases} 2 - x_1 + 3x_1^2 - x_1^3 + x_1^4 & \text{on} \quad \Gamma_1 \\ 8 + 6x_2 + x_2^2 - \min\left\{8(x_2 - 0.5)^2 + 0.58, 1\right\} & \text{on} \quad \Gamma_2 \\ 2 + 4x_1 + 3x_1^2 + 2x_1^3 + x_1^4 & \text{on} \quad \Gamma_3 \\ 2 - x_2 & \text{on} \quad \Gamma_4, \end{cases}$$

The adjoint equation is given by

$$\begin{aligned} -\Delta\phi(x) + c(x)\phi(x) &= y_u(x) - y_\Omega(x) \qquad \text{in} \quad \Omega \\ \partial_\nu\phi(x) + \phi(x) &= e_y(x) - 2y(x)\phi(x) \quad \text{on} \quad \Gamma. \end{aligned}$$

Again a short calculation shows that

$$\bar{u}(x) = \begin{cases} x_1^3 & \text{on} \quad \Gamma_1 \\ \min\left\{8(x_2 - 0.5)^2 + 0.58, 1\right\} & \text{on} \quad \Gamma_2 \\ x_1^2 & \text{on} \quad \Gamma_3 \\ 0 & \text{on} \quad \Gamma_4 \end{cases}$$

denotes the optimal control with corresponding optimal state $\bar{y}(x) = 1 + x_1^2 + x_1 x_2$ and adjoint $\bar{\phi}(x) = -1$.

	Casas	Mateos	This	Paper	Casas	Mateos	This	Paper
h	$E_{u_{L^2}}$	$E_{u_{L^\infty}}$	$E_{u_{L^2}}$	$E_{u_{L^\infty}}$	$eoc_{u_{L^2}}$	$eoc_{u_{L^\infty}}$	$eoc_{u_{L^2}}$	$eoc_{u_{L^\infty}}$
2^{-0}	-	-	1.13e-2	1.83e-2	-	-	-	-
2^{-1}	-	-	4.72e-3	6.43e-3	-	-	1.26	1.51
2^{-2}	-	-	1.33e-3	2.19e-3	-	-	1.82	1.55
2^{-3}	-	-	3.45e-4	6.69e-4	-	-	1.95	1.71
2^{-4}	8.5e-3	4.1e-2	8.75e-5	1.89e-4	-	-	1.98	1.82
2^{-5}	3.0e-3	1.5e-2	2.20e-5	5.11e-5	1.5	1.5	1.99	1.89
2^{-6}	1.1e-3	1.1e-2	5.50e-6	1.33e-5	1.4	0.4	2.00	1.94
2^{-7}	3.8e-4	3.8e-3	1.38e-6	3.42e-6	1.5	1.5	2.00	1.96
2^{-8}	1.4e-4	2.7e-3	3.44e-7	8.66e-7	1.4	0.5	2.00	1.98
2^{-9}	-	-	8.61e-8	2.18e-7	-	-	2.00	1.99
2^{-10}	-	-	2.15e-8	5.47e-8	-	-	2.00	1.99

Table 2: Errors in u for the semilinear example

For the numerical solution of the present example again a semi-smooth Newton method is applied. Since we are dealing with nonlinear state equations the determination of u^{new} in (4.15) has to be replaced by

$$(\alpha g I + g B^* p_h'(u) g) u^{new} = -g B^* (p_h(u) - p_h'(u)(u - \beta)), \text{ and } u^{new} = \text{bounds on } \Omega \setminus \mathcal{I}(u).$$

The numerical results are very similar to that of the previous example. This is due to the fact that the nonlinearity in the state equation is monotone.

The errors and eocs for the present example are shown in table 2 for the Casas-Mateos-ansatz and the variational discretization respectively. The eoc of the numerical experiments of Casas and Mateos is calculated from tables of [2]. The eoc of the numerical experiments of Casas and Mateos is 1.5 and about 1.0 for the L^2 and L^∞ norm respectively. The eoc is 2 for our approach. This again is better than expected by Example 3.3, 1, but the same arguments as used in the previous example may justify also convergence order 2. We further note that also for this example already the errors on the coarsest mesh for $h = 1$ are smaller in our approach than than those for $h = 2^{-4}$ in the conventional Casas-Mateos-ansatz.
The terminated conditions are the same as in the previous example.
In figure 2 the optimal control together with the error for $h = 0.5$ and the finite element grid is shown.

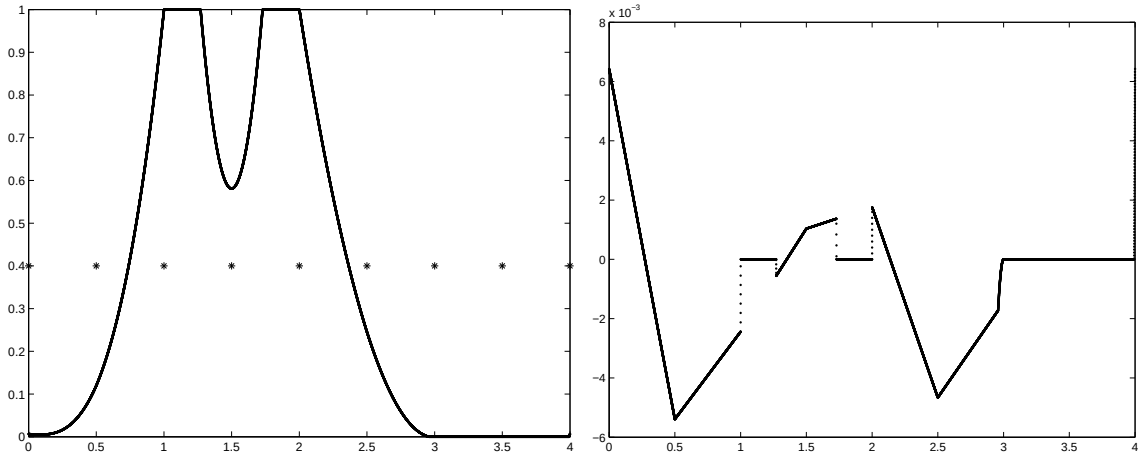

Figure 2: Optimal control u left, error in u right, both for $h = 0.5$

Acknowledgements

The first author gratefully acknowledges the support of the DFG Priority Program 1253 entitled Optimization With Partial Differential Equations.

References

[1] Casas, E., Raymond, J.P.: *Error Estimates for the Numerical Approximation of Dirichlet Boundary Control for Semilinear Elliptic Equations*, Siam J. Control Optim. 45, 1586-1611, (2007)

[2] Casas, E., Mateos, M.: *Error Estimates for the Numerical Approximation of Neumann Control Problems* , Comp. Appl. Math., to appear.

[3] Casas, E., Mateos, M., Tröltzsch, F.: *Error Estimates for the Numerical Approximation of Boundary Semilinear Elliptic Control Problems*, Preprint 2003/21 TUB August 2003

[4] Deckelnick, K., Hinze, M.: *Convergence of a finite element approximation to a state constrained elliptic control problem*, Siam J. Numer. Anal. 45:1937-1953 (2007)

[5] Deckelnick, K., Günther, A, Hinze, M.: *Boundary control of elliptic equations in smooth domains*, in preparation, 2008.

[6] Hintermüller, M., Ito, K., Kunisch, K.: *The primal-dual active set method as a semi-smooth Newton method*, Siam J. Control and Optim., 13 pp. 865–888, (2003).

[7] Hinze, M.: *A variational discretization concept in control constrained optimization: the linear-quadratic case*, J. Computational Optimization and Applications **30**, 45-63 (2005).

[8] Hinze, M., Pinnau, R., Ulbrich, M., Ulbrich, S.: *Modelling and Optimization with Partial Differential Equations*, Lecture Notes of the Autumn School with same title, Hamburg, 2005, to appear with Springer.

[9] Hinze, M., Vierling, M.: *Semi–discretization and semi-smooth Newton methods; implementation, convergence and globalization in pde constrained optimization with control constraints*, Preprint, to appear (2008).

[10] Schatz, A.H.: *Pointwise error estimates and asymptotic error expansion inequalities for the finite element method on irregular grids. I: Global estimates*, Math. Comput. 67, No.223, 877–899 (1998).

[11] Ulbrich, M.: *Semismooth Newton Methods for Operator Equations in Function Spaces*, Siam J. Optim. 13, 805–841 (2003).

[12] Vexler, B.: *Finite Element Approximation of Elliptic Dirichlet Optimal Control Problems*, Numerical Functional Analysis and Optimization, Vol. 28(7-8), 957 - 973, (2007)

[13] Xu, J., Zou, J. : *Some nonoverlapping domain decomposition methods*, Siam Rev., 40:857–914, (1998).